INSTITUTE OF PLASMA PHYSICS

NAGOYA UNIVERSITY

RESEARCH REPORT

NAGOYA, JAPAN

Tokamak Experiment in SPAC-II

Yasuji Hamada* and Akihiro Mohri

IPPJ-188 March 1974

Further communication about this report is to be sent to the Research Information Center, Institute of Plasma Physics, Nagoya University, Nagoya, JAPAN.

---

* Now at Gulf General Atomic Company, La Jolla. San Diego, California, USA on leave from Institute of Plasma Physics, Nagoya University.

Synopsis

A small scale tokamak type device named SPAC-II was constructed for the investigation of various problems in the confinement and heating of toroidal plasmas. In a tokamak mode experiment, plasma with the electron temperature of 180 eV is generated, when the plasma current is 18 kA and the safety factor q = 3.9. The energy confinement time is about 200 μs which fits the scaling law of (plasma radius)^2 × (poloidal field). The current density is estimated to be 4×10^2 A·cm^{-2} for the parabolic distribution.

1. Introduction

Tokamak is now the most promising apparatus to show a thermonuclear fusion feasibility. It still contains many problems to be solved beforehand, i.e. M.H.D. equilibrium and stability at lower q value[1], plasma transport in collisionless regime[2] and various further heating to get the ignition of fusion[3]. Also the stationary driving of the plasma current is more profitable.

Hitherto, high temperature plasma in tokamak has been obtained only in large scale apparatus such as T-3[3], T-4[4], TM-3[5], ST[6], JFT-2[7] and TFR[8]. In this report it is shown that even in a small scale tokamak we can obtain a high electron temperature plasma if some attentions are paid to the design of apparatus and its operation. Owing to the strong toroidal magnetic field and the small major radius, high current density of ohmic heating can be obtained. At this high current density ($2.5 \sim 5 \times 10^2$ A$\cdot$cm^{-2}), the anomalous electrical resistivity of the plasma is not observed. The energy confinement time τ_E is still governed by the relation $a_p^2 B_p$ where a_p is the plasma radius and B_p the poloidal magnetic field.

2. Experimental Apparatus

A toroidal device named SPAC-II is constructed, the basic design of which is mainly derived from tokamak. It has an aluminum shell of 1.5 cm thick and a liner made of a stainless steel bellows with thickness of 0.3 mm. The major radius of the torus is 28 cm and the inner radius of a molybdenum diaphragm limiter is 5.5 cm. The clearance between the inner side of the limiter and the inner surface of the shell is 2.5 cm. A transverse slit of the shell is made as narrow as 4 mm to ensure the toroidal symmetry. Toroidal magnetic field coils, each of which has 11 turns hollow conductor windings, are energized by the discharge of a 250 kJ capacitor bank, and the maximum field at the minor axis is 20 kG. A quasi-steady vertical field is available up to 200 G. An iron core transformer for driving the plasma current is made of 0.3 mm thick cold-milled oriented silicon steel. Its cross section is circular near the toroidal centre and rectangular at other portion. The core is usually dc biased to have large flux swing (0.09 V·sec). The primary windings for ohmic heating are wound on the upper and the lower sides of the centre-leg of the core. A capacitor bank is connected through an adjustable resister to the primary windings. By changing the capacity and the resistance, the most appropriate condition for the plasma discharge can be found. The liner is evacuated by a turbo-molecular pump below the pressure of 3×10^{-7} torr. Hydrogen gas is fed as the working gas through a leak volve. The schematic diagram of the experimental set-up is shown in Fig.1, and parameters of SPAC-II are also summarized in Table 1.

Table 1. Parameters of SPAC-II apparatus

Major radius of the torus:		28 cm
Diaphragm limiter:	material	molybdenum of 1.5 mm thick
	inner radius	5.5 cm
Liner:	material	stainless steel bellows of 0.3 mm thick
	inner radius	6.7 cm
Shell:	material	aluminum of 1.5 cm thick
	inner radius	8 cm
Transformer:	material	cold-milled oriented core of 0.3 mm thick
	flux swing	0.09 V•s
Vacuum:	base pressure	$< 3 \times 10^{-7}$ Torr
	pump	turbomolecular pump
Toroidal magnetic field:		$\leq$ 20 kG
Vertical magnetic field:		$\leq$ 200 G
Compensating horizontal field:		$\leq$ 50 G

Between the shell and the liner, 24 magnetic search coils, two Rogowski coils and a loop coil are installed for various electromagnetic measurements. The electron temperature is inferred from the Thomson scattering measurement with a 3 J-100 MW ruby laser. The electron density is estimated from the comparison between the Thomson scattering of plasma and the Rayleigh scattering of nitrogen gas.

3. Experimental Results

3.1 Discharge cleaning

The preconditioning by discharge cleanings is essential to obtain a high temperature plasma. In SPAC-II, the discharge cleaning is performed by driving the plasma current under the weak toroidal magnetic field of 2.5 kG and the fairly high loop voltage of 150 V.

After about 800 discharges, the plasma current begins to grow above the Kruskal-Shafranov limit without violent fluctuations in the loop voltage. The safety factor q is reduced to about 0.4. Then, after 1000 discharges, the current decreases whence violent positive spikes appear in the loop voltage. Finally, after 1200 discharges, a large positive spike train blocks the rise of the plasma current above the Kruskal-Shafranov limit, as shown in Fig.2. In the subsequent discharges, the loop voltage and the plasma current wave forms do not change appreciably compared with those shown in Fig.2.

The usual discharge characteristics of tokamak mode can be realized after above mentioned preconditioning. In this case, the series resistance and the capacity of the ohmic heating circuit are appropriately chosen, and the compensation of the stray magnetic field is also required.

3.2 Compensation of the stray magnetic field

The presence of the stray major-radial (horizontal) magnetic field often deteriorates the plasma parameter in tokamak[9]. The stray field originating in the toroidal coils and the iron-core transformer is compensated by imposing a quasi-dc horizontal field. The stray horizontal field is inferred from the measurement of the breakdown time of the gas. Figure 3 shows typical wave forms of the plasma current and the loop voltage, and there the breakdown time is also indicated. The dependence of the breakdown time upon the dc horizontal magnetic field is shown in Fig.4. From the measurement of the vertical shift of plasma column with the magnetic search coils, it is found that the optimum horizontal field strength lies on the value at which the breakdown time is minimized. The optimum horizontal field changes its sign as the toroidal magnetic field is reversed. The ratio of the horizontal stray magnetic field B_h to the main toroidal field B_t is $B_h/B_t \simeq 2.6 \times 10^{-3}$.

3.3 Discharge characteristics

Negative spikes and cooperative phenomena

Under the weak toroidal field, B_t = 10.5 kG, the plasma becomes unstable if q value are reduced below 5. Figure 5 shows the occurence of the negative spikes in the loop voltage V_l in conditions $q < 5$. When the spikes appear, the plasma current I_p decreases and the overall loop voltage increases. The time relation between the occurence of the spike and the emission of CIII 4561 Å is shown in Fig.6. We can see that this impurity line increases step-wise, correlating with the spikes. These facts imply that the discharge is deteriorated by the spikes. As can be seen from Fig.5, at $q > 5$, we can get a stable and fairly high temperature plasma. The radiations of impurity lines CIII 4561Å and OIII 3759 Å in this case are shown in Fig.7. Both line emissions last only 300 μs from the breakdown of the gas and they become again radiative as the loop voltage becomes larger at the end of discharge.

Abrupt destruction of plasma column near $q_a = 2$

The safety factor q can be changed with time from higher value to lower one when the duration of plasma current is prolonged to a comparable time with the decaying time of the toroidal magnetic field. The toroidal magnetic field is generated with a somewhat smaller capacitor bank, and the RC time constant of the ohmic heating circuit is set to be longer. The ohmic heating voltage is applied at the peak of the magnetic field (10 kG). In this case, the decay rate of the toroidal field becomes faster than that of the plasma current. Figure 8 shows the time dependences of the plasma current, the loop voltage and the magnetic field. Here, the associated safety factor q_a estimated at the radius of 4.5 cm is also indicated. As the magnetic field decreases, sharp positive spikes in the loop voltage appear successively which well correlated with $q_a = 6, 5, 4, 3$. Finally, near $q_a = 2$, the plasma abruptly collapses, followed with a large increase of the loop voltage.

It is clear that the lower q than 2 is difficult to be realized from the state $q > 2$.

State of high current density

Low q value and higher conductivity temperature can be obtained at stronger toroidal magnetic field. Figure 9 shows typical discharge wave forms of the loop voltage V_l and the plasma current I_p at $B_t = 14$ kG. The plasma current is 18 kA at maximum, whence the safety factor at the plasma periphery $q_a = 3.9$. The electron temperature on the minor axis is measured by the Thomson scattering of the ruby laser light, the total energy of which is 3 J. For the suppression of the stray light level, a color glass is installed inside the chamber as a view damp. Figure 10 shows the dependence of scattered signals upon the square of wavelength displacement, $(\Delta\lambda)^2$, in the discharge shown in Fig.9. This scattering measurement is performed about 300 μs after the current peak. The estimated electron temperature is 180 eV. Also by comparing the signals of the Thomson scattering and of the Rayleigh scattering, the plasma density at the minor axis is estimated to be 2.5×10^{13} cm^{-3}.

We suppose that the plasma density profile is like parabolic, $n(r) \propto 1 - (r/a)^2$, where a is the inner radius of the limiter and that the ion energy density is negligible compared with that of electrons. Then, we can obtain the energy confinement time by the equation

$$\tau_E = \frac{NkT_e}{I_p V_l}$$

under the condition $dI_p/dt = 0$, where N is the total number of electrons. Here, it is also assumed that the inner inductance of plasma is not changed appreciably. Using the parameters of the discharge at the current peak; $I_p = 18$ kA and $V_\ell \simeq 1.5$ V, and assuming that the density and the electron temperature are the same as at 300 μs after; $n(0) \simeq 2.5 \times 10^3$ cm^{-3} and $kT_e \simeq 180$ eV, we have $\tau_E \simeq 200$ μs. In this case, the poloidal magnetic field, B_p, at $r = a$ is 6.5×10^2 G and the poloidal β-value (ratio of the plasma pressure to the pressure of the poloidal magnetic field), β_p, is 0.36. According to the scaling law of $\tau_E \propto a^2 B_p$ proposed by Grobunov et al[10], τ_E is calculated to be 300 μs in our case. Thus, the energy confinement time of plasma in SPAC-II fits the $a^2 B_p$ scaling law within factor of 2.

The current density $j(r)$ is also deduced under a reasonable assumption of its profile. In case of the palabolic distribution $j(0)$ becomes 4.2×10^2 $A \cdot cm^{-2}$, whereas $j(0) = 2.1 \times 10^2$ $A \cdot cm^{-2}$ for the flat distribution. For the parabolic distribution, the electron drift velocity due to the current $U_d = j/en$, where e is the electron charge, becomes 1×10^8 cm·s^{-1}, and the ratio U_d/v_s ($v_s = \sqrt{kT_e/m_i}$ is the ion sound velocity) is 10. Thus, we can expect the appearance of the "amomalous" resistivity[11). However, the conductivity temperature in case of the parabolic distribution is estimated to be about 240 eV for ions of unit charge i.e. Z = 1. Even in usual large scale tokamak, the effective value of Z is greater than unity. It can not be expected that the plasma in SPAC-II is very clean and multiply-charged ions do not affect the conductivity temperature. Therefore, other attributions should be considered to explain there is no remarkable anomalous resistivity. One of them might be the presence of runaway electrons. In fact, hard X-rays are observed. Energy spectral measurements of X-rays are under preparation.

4. Conclusion

We have shown that some behaviours of plasma, which have been observed in large scale tokamak devices, can be realized even in a small device. In order to get such a result, deep attentions should be paid to the accuracy of magnetic field, the oil-free vacuum and the sufficient preconditioning.

The main results are as follows:

1) A large periodic positive-spike train is observed when the plasma current is impeded to grow above the Kruskal-Shafranov limit.
2) A new simple method is proposed for measuring the stray magnetic field. The variation of the break-down time with the external compensating magnetic field is very sensitive. The condition to minimize this time corresponds to the optimum compensation.
3) At the decaying phase of the toroidal field, the positive spikes of the loop voltage are observed near $q_a = 5, 4, 3$. Then, the plasma collapses near $q_a = 2$.
4) Even in the small scale apparatus, plasma with high electron temperature is obtainable and the energy containment time fits the scaling law of a^2B_p which has been obtained in large apparatus.
5) The obtained current density is raised to 400 $A \cdot cm^{-2}$, at which remarkable anomalous resistivity is not observed. At this high current density, the contribution of runaway electrons would be taken into account.

Acknowledgement

The authors would like to express their sincere thanks to Mr. S. Fujiwaka for the help of design, Emeritus Prof. K. Husimi and Prof. R. Itatani for continuous encouragement. Prof. N. Inoue and Mr. K. Matsuoka supported the experiment. Thanks are also due to Mr. K. Ukegawa and Mr. T. Kato for help of the operation. It should be noted that Prof. K. Hirano and Mr. S. Kitagawa prepared the capacitor bank system with high reliability.

References

1) L. A. Artsimovich; Nucl. Fusion 12 (1972) 215.

2) B. B. Kadomtsev and O. P. Pogutse; Nucl. Fusion 11 (1971) 67.

3) A. M. Anashin et al; Soviet Physics-JETP 33 (1971) 1127.

4) L. A. Artsimovich, et al; Nucl. Fusion, Spec. Suppl. (1972) 41.

5) G. A. Bobrovskii, et al; Soviet Physics-JETP Letters 9 (1969) 158.

6) D. Dimock et al; Plasma Physics and Controlled Nuclear Fusion Research, 1971 (IAEA, Vienna, 1971) I, p.451.

7) S. Itoh et al; 3rd Symposium on toroidal plasma confinement, Garching, March 1973-B4.

8) The T.F.R. Group, 6th European Conference on Controlled Fusion and Plasma Physics, 1973-July.

9) L. A. Artsimovich et al; Soviet Atomic Energy 17 (1964) 886.

10) E. P. Gorbunov, S. V. Mirnov and V. S. Strelkov; Nucl. Fusion 10 (1970) 43.

11) L. I. Rudakov and E. K. Zavoisky; Atomn. Energ. 23 (1967) 417.

Figure Captions

Fig.1. Schematic diagram of SPAC-II.

Fig.2. Discharge characteristics during discharge cleaning.
B_t = 2.5 kG, filled gas pressure $p = 1 \times 10^{-3}$ torr(H_2),
upper trace: loop voltage V_ℓ (20 V/div.),
lower trace: plasma current I_p (10 kA/div.),
sweep rate: 0.5 ms/div..

Fig.3. Typical discharge waveforms at B_t = 14 kG.
$p = 4 \times 10^{-3}$ torr,
upper trace: I_p (7.7 kA/div.),
lower trace: V_ℓ (10 V/div.),
sweep rate: 0.2 ms/div..
The break down time τ_{BD} is defined.

Fig.4. Breakdown times versus DC horizontal field.
$B_t = \pm 14$ kG, $p = 4 \times 10^{-4}$ torr.

Fig.5. Negative spikes which limit the plasma current above q = 5.
B_t = 10.5 kG, $p = 4 \times 10^{-4}$ torr(H_2).
upper trace: V_ℓ (20 V/div.),
lower trace: I_p (7.7 kA/div.),
sweep rate: 0.5 ms/div..
At the peak of plasma current,
(a) q = 5.5, (b) q = 4.5, (c) q = 2.8, (d) q = 2.5.

Fig.6. Correlation between the negative spike and the emission of CIII (4561 Å). The discharge condition is the same as in Fig.5(b).
sweep rate: 20 μs/div..

Fig.7. Emissions of CIII (4561 Å) and OIII (3759 Å).

B_t = 10.5 kG, p = 4 × 10^{-4} torr(H_2), q = 5.5.

upper trace: V_ℓ (5 V/div.),

middle trace: I_p (5 kA/div.),

lower trace: signal from the monochrometer,

sweep rate: 0.5 ms/div..

Fig.8. Characteristics of the long discharge at the fading stage of the toroidal magnetic field.

B_t = 10 kG at peak, p = 2.7 × 10^{-4} torr(H_2),

V_ℓ: 5 V/div., I_p: 10 kA/div., sweep rate: 1 ms/div..

The safety factor q_a is estimated at the minor radius of 4.5 cm.

Fig.9. Typical waveforms of the discharge at higher magnetic field.

B_t = 14 kG, $p \simeq 3 \times 10^{-4}$ torr(H_2), I_p = 18 kA at peak (q = 3.9),

upper trace: I_p (7.7 kA/div.),

lower trace: V_ℓ (10 V/div.),

sweep rate: 0.2 ms/div..

Fig.10. Logarith of the scattered signal of the laser light as a function of the square of the wavelength displacement, $(\Delta\lambda)^2$. The condition of the discharge is the same as in Fig.9. The measurement is done 300 μs after the current peak.

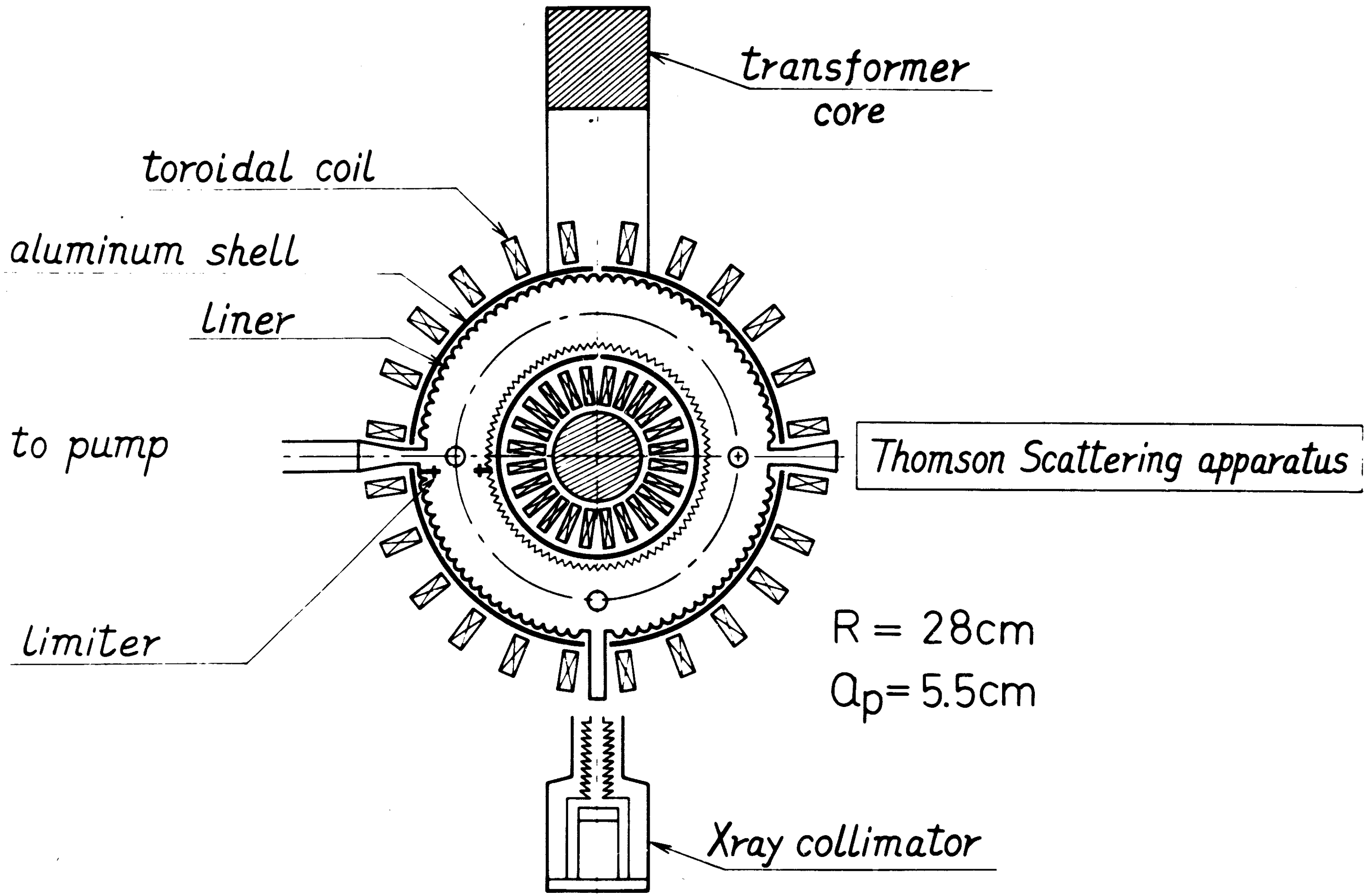

Fig.1 Schematic Diagram of SPAC II

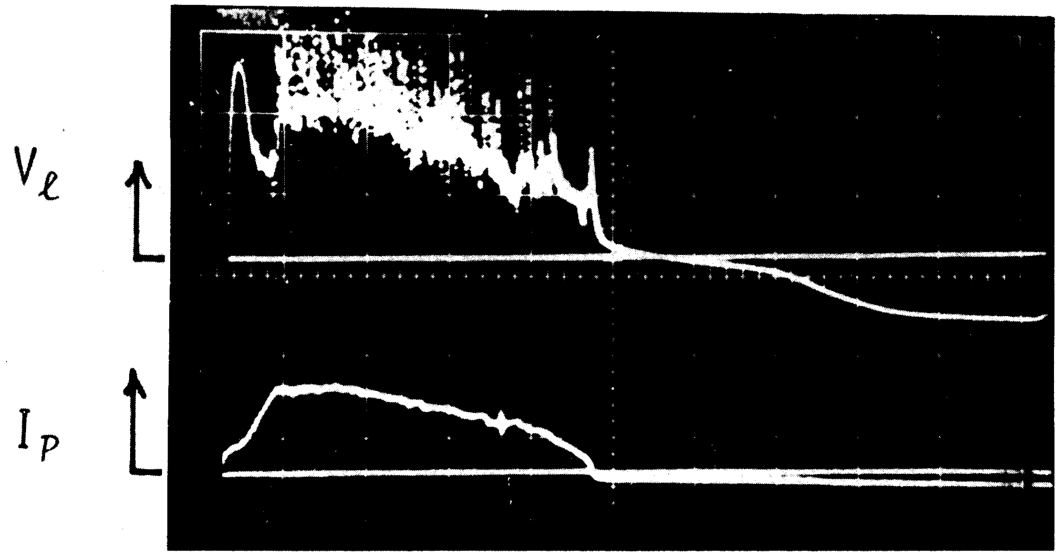

FIG. 2

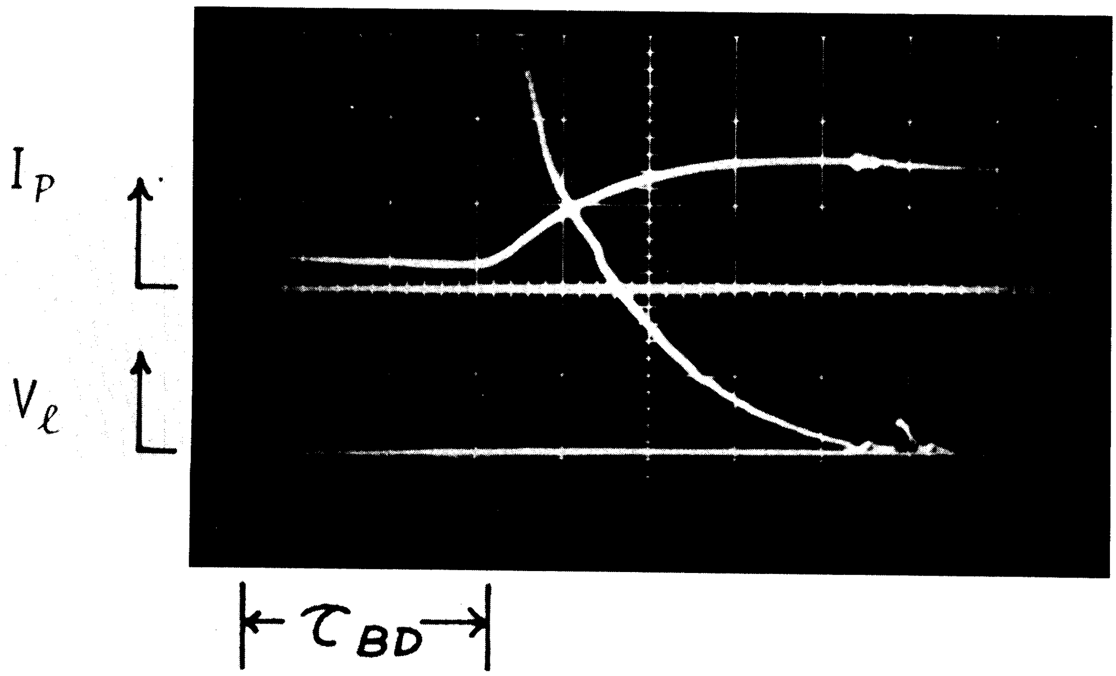

FIG. 3

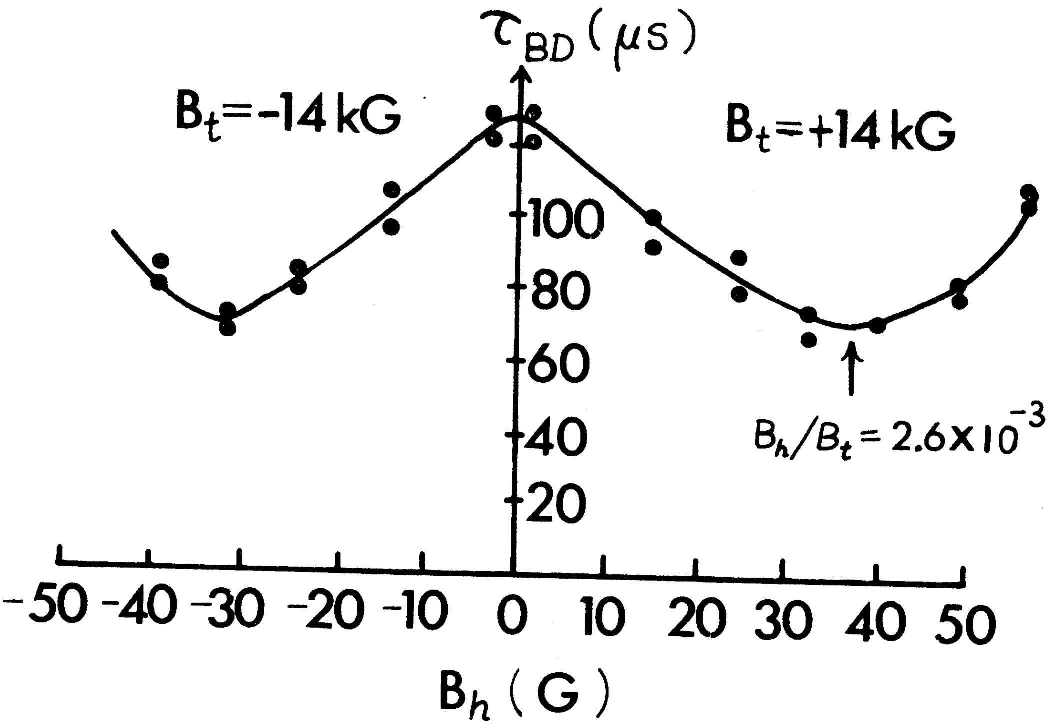

τ_{BD} (μs)
B_t=-14 kG
B_t=+14 kG
100
80
60
40
20
B_h/B_t = 2.6X10^{-3}
-50 -40 -30 -20 -10 0 10 20 30 40 50
B_h (G)

FIG. 4

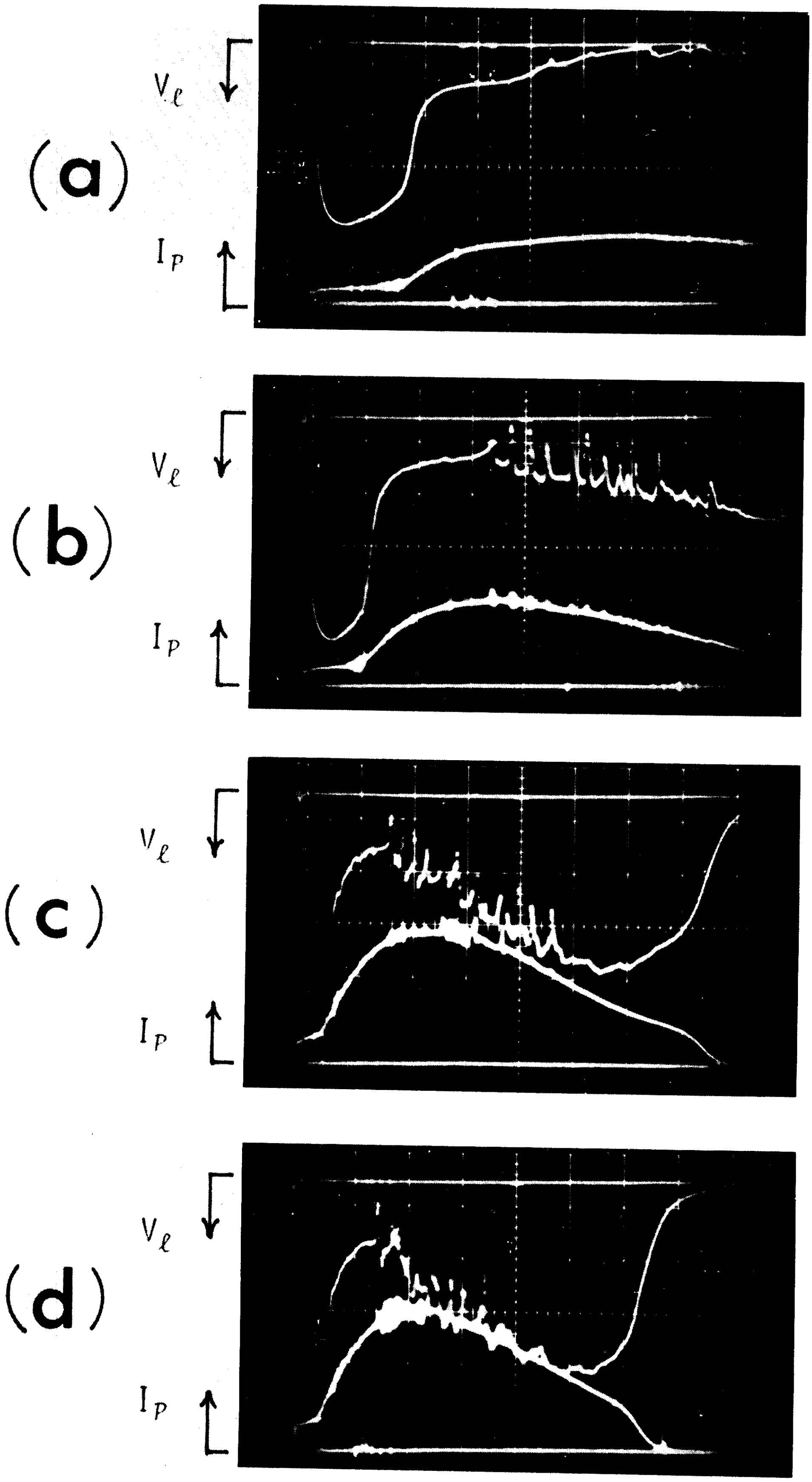

FIG. 5

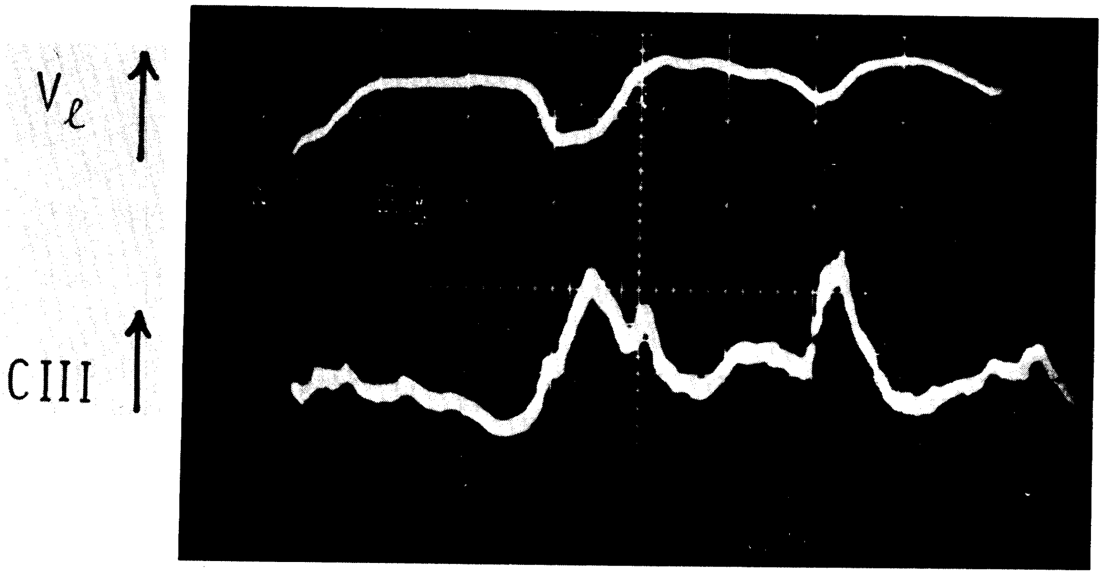

FIG. 6

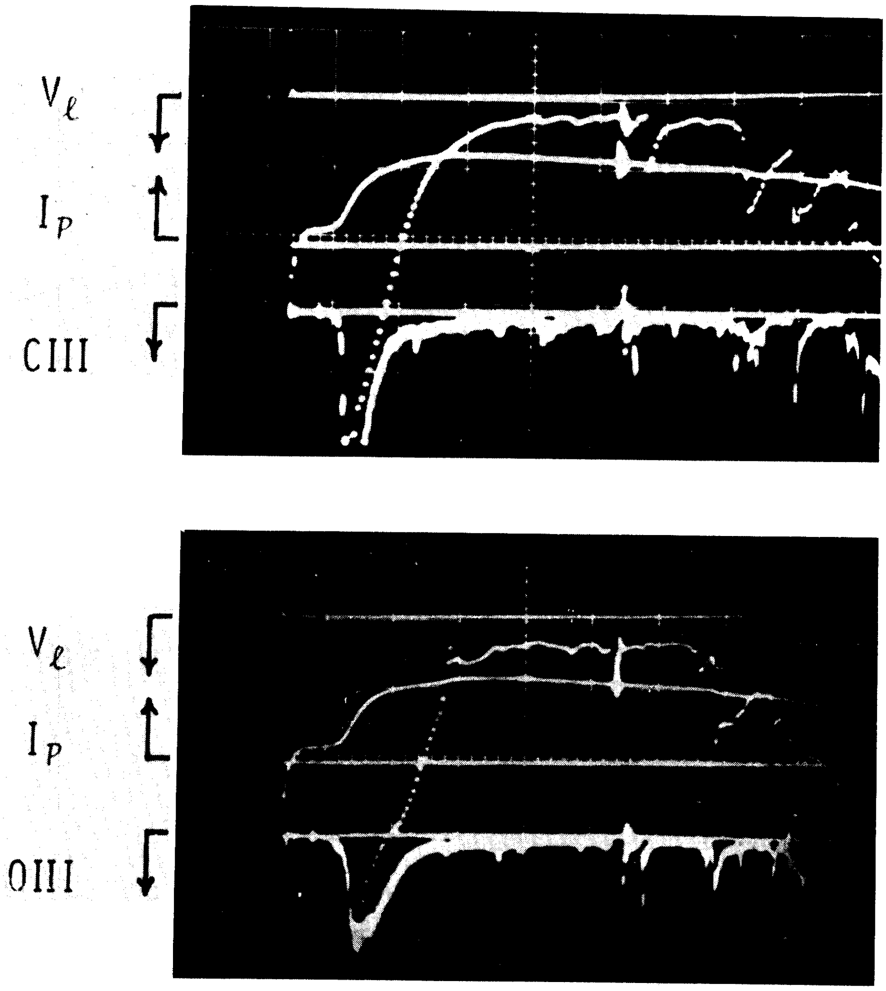

FIG. 7

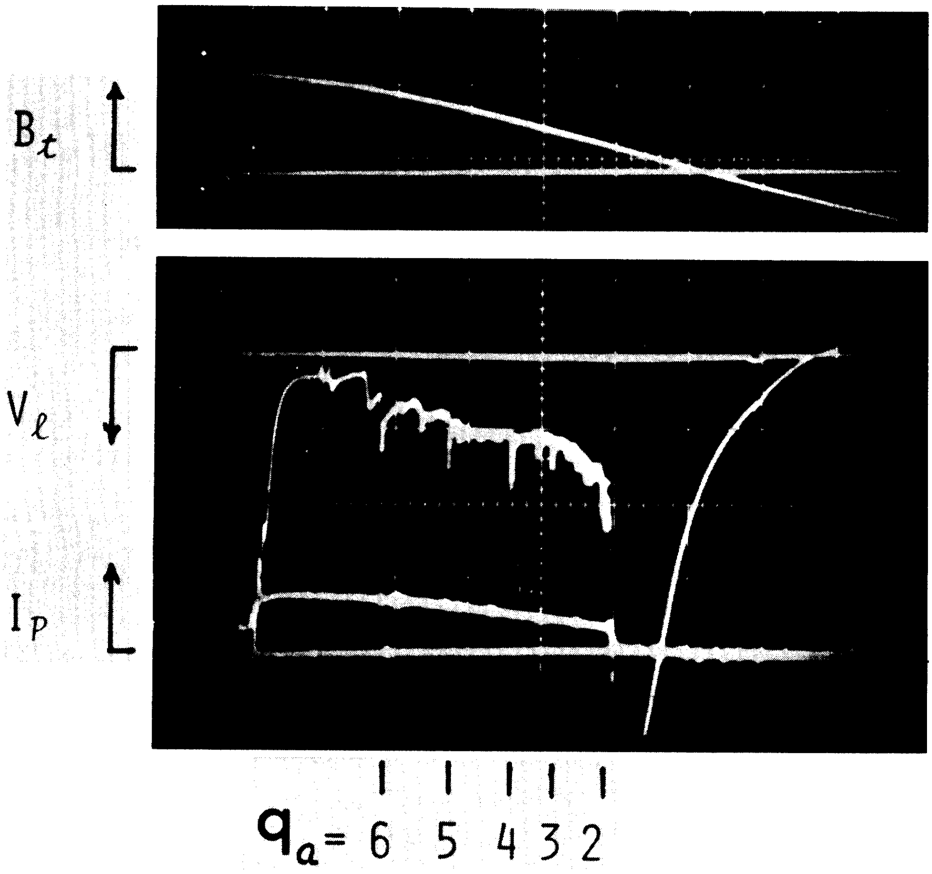

FIG. 8

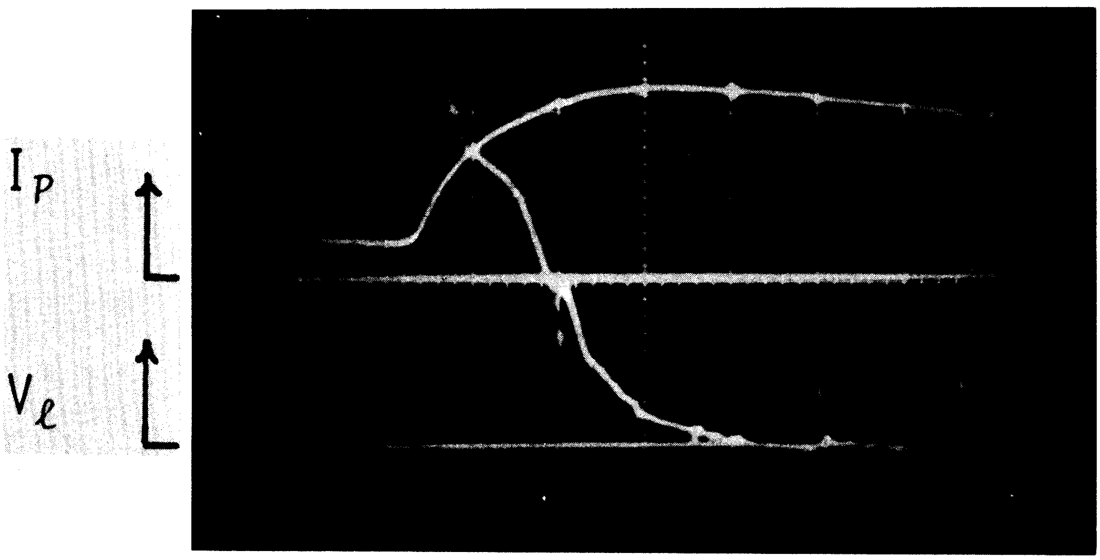

FIG. 9

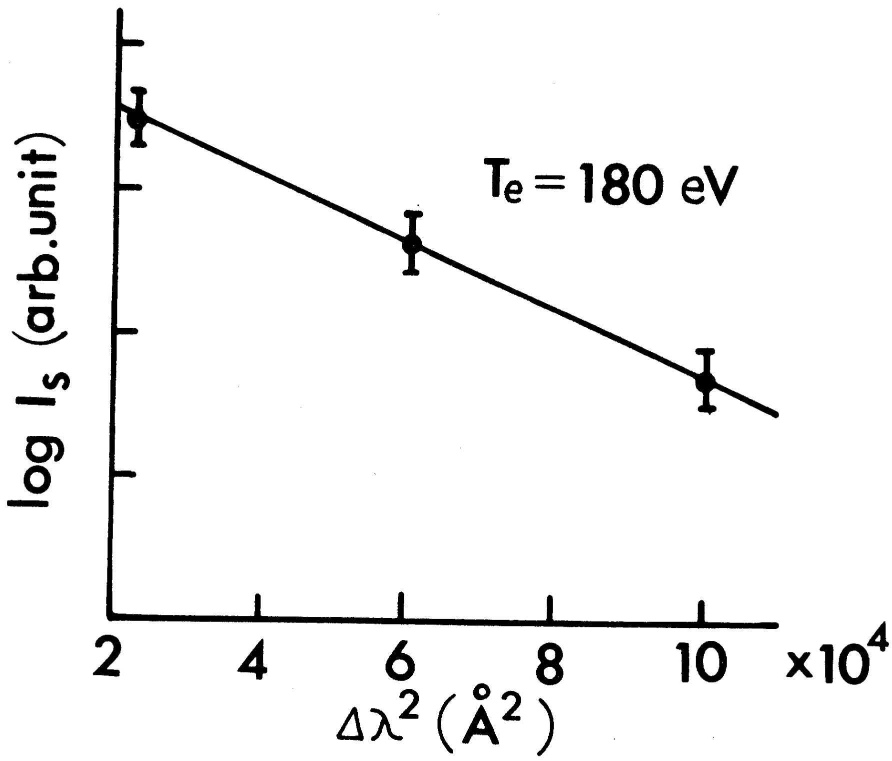

FIG. 10